ALMA Memo 395

Alignment Tolerances for ALMA Optics

B.Lazareff
IRAM
25-Oct-2001

Abstract

A tolerance analysis of the alignment of the ALMA FE optics is presented. The following performance criteria are taken into account: a) loss of on-axis efficiency from aperture plane misalignment; b) focal plane co-alignment of the two beams of each band; c) aberrations when off-axis mirrors operate between wavefronts not centered on the foci of the ellipsoid; d) non-uniform phase across the primary beam resulting from aperture plane misalignment.
It is found, based on reasonable machining tolerances, and existing FEM simulations of pressure bending, that the adopted goals can be met, the driving goals being on-axis efficiency (a) and primary beam phase (d).
The present study, especially in view of the fact that detailed designs of cartridge internal optics do not exist at the time of writing, can ***only be considered as a guideline****. The author cannot take responsibility for the fact that a particular cartridge will or will not meet alignment specs, based on, e.g., tolerances written on fabrication blueprints that do not yet exist. Some assumptions had to be made concerning accuracies used as input in the calculation, that need to be confirmed by the groups respectively in charge.*

1. Introduction

Through the efforts of several ALMA teams, an optical configuration has been designed with the goal of optimizing its efficiency, taking into account requirements or constraints from other areas, notably cryogenics. The geometrical optical design is about to be finalized. Due to small fabrication errors and environmental factors (gravity, thermal, etc), the front-end as-built will inevitably deviate from the ideal design. It is therefore necessary, before the detailed design is undertaken, to quantify the impact of deviations between the actual and designed optics against the system performance specifications. Then, a tolerance budget can be divided up between subsystems and components, so that fabrication techniques and control procedures can be designed to meet the system specifications.

For the purpose of the present analysis, the reference optical design is the one described in ALMA Memo 362 (Lamb et al) [1]. Fruitful discussions with P. Napier, J. Lamb, R. Lucas, and S. Guilloteau are acknowledged.

2. System specs and tolerances: outline

2.1. Specifications

The present study is driven by two specifications, neither of which is explicitly part of the project specifications:

- Minimal loss of optical efficiency of the actual front-end, compared with the design. A nominal criterion of 1% efficiency loss is used.
- Deviations from flat phase in primary beam consistent with the requirement for amplitude errors: pointing accuracy 6% of HPBW, as specified in Table 2.1, Chapter 2 of the ALMA Project Book [2], and resulting in an antenna specification of 0.6" pointing error. Note that the pointing accuracy refers to random errors, while the primary beam phase pattern, in principle, is stable and can be calibrated.

These will be discussed in more detail further down.

2.2. Impact of misalignments

Mechanical misalignments cause the parameters of the beam illuminating[1] the secondary to deviate from their nominal values. Such deviations will be reckoned in the telescope focal plane and can be classified as:

1) Displacement
   a) Along telescope axis
   b) Lateral shift in focal plane (= tilt in aperture plane, = pointing offset on the sky)
   c) Tilt in focal plane (= lateral shift in aperture plane, =loss of aperture efficiency)
   d) Rotation about telescope axis
2) Distortion (coupling to higher order modes, if the launched beam is fundamental gaussian) within the front-end optics.

Effect 1a is not considered here, because even in the nominal design, the various bands are not constrained to have a common focus, as long as the amount of spherical aberration associated with refocusing is tolerable (see Memo 362). Effect 1b is considered only insofar as concerns the co-alignment of the two orthogonally polarized beams of one band; the common pointing offset needs to be calibrated for each band anyway. Effect 1c is the dominant one in the present study. Effect 1d is weighed by the sine of the small angle between each beam and the telescope axis, and can be ignored if a reasonable level of general tolerance is maintained. Effect 2 will be addressed, but it will be found that it is not driving the tolerances.

2.3. Interplay of misalignments and specifications

This can be summarized graphically:

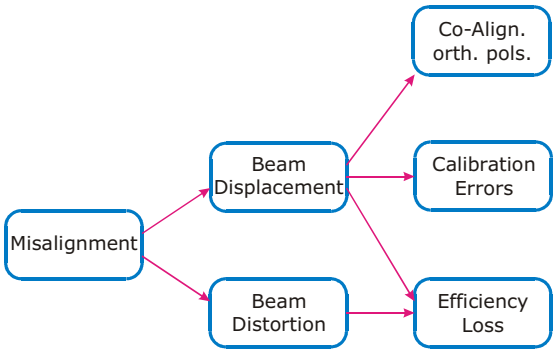

Figure 1: Flow diagram from misalignements to optical properties

[1] As is common practice, I regard the optics and telescope working as a transmitter.

3. Efficiency loss from beam deviation

Based on a gaussian illumination with a 12dB edge taper, one finds that a 1% drop of on-axis efficiency is reached when the illumination pattern is offset from the center of the secondary by $0.088 \times r_s$. This corresponds to an angular offset of 5.5mrad from the nominal launch angle in the focal plane. I rounded this up to 6mrad (1.2% efficiency loss). The actual edge taper found from the electromagnetic analysis of Tham and Withington [3] (P.O. analysis available for bands 3–6, and 9 at the time of writing) lies between 10.5 and 11.9dB; it was felt that the discrepancy did not warrant a re-evaluation of the tolerance criterion.

I use the ABCD equations of geometrical optics to propagate the perturbation of the chief ray; one can show that the same equations apply to the main axis of a gaussian beam. It is assumed that the unperturbed optical path is contained in a plane, and only perturbations of the chief ray within that plane are computed, which simplifies the work while still providing a first approach at an estimate of tolerances.

A summary of the method is given in Appendix A.

3.1. Results: Sensitivity to individual misalignments

In a first step, the sensitivity of the position to *individual* misalignments is computed. Both linear and angular misalignments are considered, in the plane of the folded optical path (or in an arbitrary plane for bands 1 & 2). Also two types of misalignments are considered:

- Independent displacement of an optical element;
- A "break", i.e., all elements from the feed up to some element in the optical train are perturbed, the other elements remaining unperturbed. This covers, as a particular case, the global misalignment of a cartridge (bands 5-10).

Although both the lateral and angular displacements of the beam at the focal plane are computed, the former is so small that it is negligible as concerns the aperture plane alignment, and only the angular displacement is considered in this part of the analysis. The results are summarized in graphical form in figures 2 and 3.

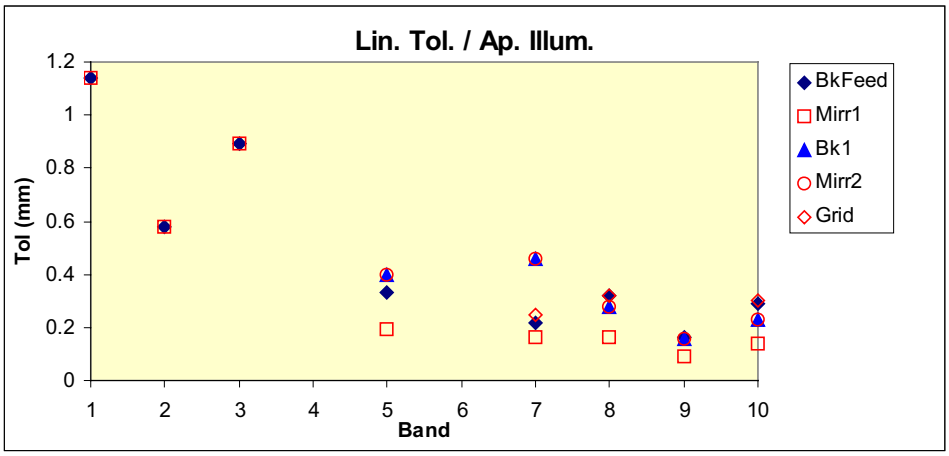

Figure 2: Tolerances for linear *displacements of optical elements that would* alone *cause a 6mrad misalignment of the beam. Legend: BkFeed: "break" after feedhorn, synonymous with feedhorn displacement; Mirr1: displacement of mirror/lens #1; Bk1: "break" after lens/mirror #1 (see Figure A-1 in Appendix 1 for definition of a break); Mirr2: displacement of mirror 2; Grid: displacement of grid (if applicable).*

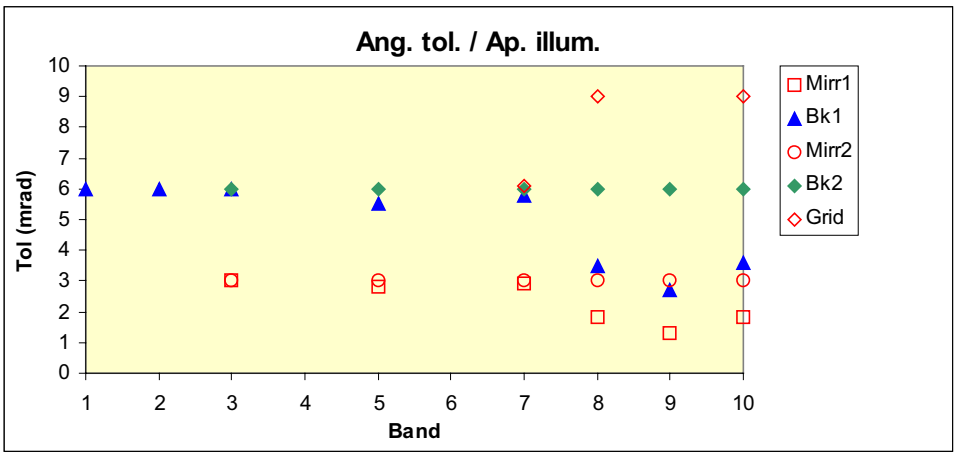

Figure 3: Tolerances for angular *displacements of optical elements that would* alone *cause a 6mrad misalignment of the beam*

3.2. Results: Global tolerance budget.

To complement the analysis presented above, I now perform a global, forward, tolerance evaluation. Reasonable (?) guesstimates are made for the accuracy with which various elements can be positioned with respect to each other, and estimates are derived for the angular deviation of the beam "emitted" by the receiver towards the secondary. In addition to the misalignments already considered, I also take into account the following:

- The cold optics elements are assumed to be mounted on some "sub-frame", which itself has a positioning accuracy w/r to the cartridge's 4K plate;
- The displacement of the 4K plate w/r to the vacuum vessel, including the pressure, gravity, and thermal deformation, and the machining accuracy;
- The misalignment, due to machining accuracy, of the back plate of the vacuum vessel (to which the cartridge is referenced), w/r to the front side interface of the vacuum vessel to the telescope;
- The misalignment between the reference frame defined by the telescope interface to the vacuum vessel, on one hand, and the line of sight to the center of the subreflector, on the other hand.

The displacement of the 4K plate w/r to the vacuum vessel due to pressure deformation of the latter is estimated from a map of deflections of the back plate, kindly provided by M.Harman (Ansys FEM calculation performed Apr 5, 2001).

- Bands 1 and 2: differential sag of the back plate: $\delta z = 0.046$ mm; cartridge diameter D = 170 mm; angular deflection: $\theta = 0.27$mrd; resulting lateral motion at distance H = 600 mm from base x = 0.16 mm.
- Bands 3 and 4: differential sag of the back plate: $\delta z = 0.080$ mm; cartridge diameter D = 140 mm; angular deflection: $\theta = 0.57$mrd; resulting lateral motion at distance H = 600 mm from base x = 0.34 mm.
- For the other bands, a value of $\theta = 0.5$mrd is used (not critical), while the linear offset is not significant because it affects the FE optics globally and amounts to a pointing offset.

The gravity deformations of the current baseline cartridge (tubular GFRP support structure, no holes) are negligible: 2.5µm linear, 8µrad.

The machining accuracy in positioning the 4K plate w/r to the vacuum vessel is guesstimated at 0.05mm, 0.2mrad.

The assumed linear and angular tolerances are multiplied by the appropriate elements of the P matrix (see above and Appendix A), and two values of the global misalignment are computed:

- Worst case: sum of absolute values;
- RSS: square root of sum-of-squares.

The geometry of the tolerancing is still only 2-D. A pessimistic estimate might be obtained by multiplying the global misalignment by $\sqrt{2}$. The results are listed in Table 1.

Table 1. Estimates of the angular misalignment of the beam coupled by the FE optics. Both worst-case and RSS estimates are given for each band.

Assume some standard values for tolerances of:

		Value	Unit	Var.					
Position of cartridge elements within cartridge optics									
	Linear	0,02	mm	CEL					
	Angular	1,0E-04	rd	CEA					
Global position of cartridge optics w/r to 4K plate									
	Linear	0,02	mm	COL					
	Angular	1,0E-04	rd	COA					
Position of cartridge 4K plate w/r to vacuum vessel									
		Pressure		Machining		Total			
Bnd 1-2	Linear	0,16	mm	0,05	mm	0,21	mm	CVL1	
	Angular	2,7E-04	rd	2,0E-04	rd	4,7E-04	rd	CVA1	
Bnd 3-4	Linear	0,34	mm	0,05	mm	0,39	mm	CVL3	
	Angular	5,7E-04	rd	2,0E-04	rd	7,7E-04	rd	CVA3	
Other	Linear	0,25	mm	0,05	mm	0,3	mm	CVL	Not Used
	Angular	5,0E-04	rd	2,0E-04	rd	7,0E-04	rd	CVA	
Positition of vacuum vessel w/r to receiver flange									
	Angular	5,0E-04	rd	VFA					
Position of receiver flange w/r to true telescope axis									
	Angular	5,0E-04		FTA					

Note: for bands 1-4, the global position error of the cartridge optics w/r to the vacuum vessel introduces an internal break in the optical train. For bands 5-10, it introduces a global misalignment of the receiver beam. Therefore, the tolerance equations are different for these two groups of bands.

For each band, the coefficients (partial derivatives) of beam exit angle versus misalignment are listed; then the individual contributions; finally the estimates "worst-case" and "rss". Note: A final factor of SQRT(2) has *not* been applied.

Band 1			Horn	Horn	Horn	Global	Global
Lin.	Coeff	rd/mm	5,3E-03	5,3E-03	5,3E-03		
	From		CEL	COL	CVL1		
	Contrib	rd	1,1E-04	1,1E-04	1,1E-03		
Ang	Coeff	rd/rd	0			1	1
	From					VFA	FTA
	Contrib	rd				5,0E-04	5,0E-04
WorstCase		***2,3E-03rd***					
RSS		***1,3E-03rd***					

Band 2			Horn	Horn	Horn	Global	Global
Lin.	Coeff	rd/mm	1,1E-02	1,0E-02	1,0E-02		
	From		CEL	COL	CVL1		
	Contrib	rd	2,2E-04	2,0E-04	2,1E-03		
Ang	Coeff	rd/rd	0			1	1
	From					VFA	FTA
	Contrib	rd				5,0E-04	5,0E-04

WorstCase ***3,5E-03rd***
RSS ***2,2E-03rd***

Band 3			Horn			Mirr1	Mirr2	Global	Global
Lin.	Coeff	rd/mm	6,7E-03	6,7E-03	6,7E-03	6,7E-03	0,0E+00		
	From		CEL	COL	CVL3	CEL	CEL		
	Contrib	rd	1,3E-04	1,3E-04	2,6E-03	1,3E-04	0,0E+00		
Ang	Coeff	rd/rd	0,024	0,024	0,024	2	2	1	1
	From		CEA	COA	CVA3	CEA	CEA	VFA	FTA
	Contrib	rd	2,4E-06	2,4E-06	1,8E-05	2,0E-04	2,0E-04	5,0E-04	5,0E-04

WorstCase ***4,4E-03rd***
RSS ***2,7E-03rd***

Band 4 Essentially identical to band 3

Band 5			Horn	Mirr1	Mirr2	Global	Global	Global	Global
Lin.	Coeff	rd/mm	0,018	0,031	0,015				
	From		CEL	CEL	CEL				
	Contrib	rd	3,6E-04	6,2E-04	3,0E-04				
Ang	Coeff	rd/rd	0,0088	2,16	2	1	1	1	1
	From		CEA	CEA	CEA	COA	CVA	VFA	FTA
	Contrib	rd	8,8E-07	2,2E-04	2,0E-04	1,0E-04	7,0E-04	5,0E-04	5,0E-04

WorstCase ***3,5E-03rd***
RSS ***1,3E-03rd***

Band 6			Horn	Mirr1	Mirr2	Global	Global	Global	Global
Lin.	Coeff	rd/mm	0,023	0,038	0,017				
	From		CEL	CEL	CEL				
	Contrib	rd	4,6E-04	7,6E-04	3,4E-04				
Ang	Coeff	rd/rd	0,01	2,79	2	1	1	1	1
	From		CEA	CEA	CEA	COA	CVA	VFA	FTA
	Contrib	rd	1,0E-06	2,8E-04	2,0E-04	1,0E-04	7,0E-04	5,0E-04	5,0E-04

WorstCase ***3,8E-03rd***
RSS ***1,4E-03rd***

Band 7			Horn	Mirr1	Grid	Mirr2	Global	Global	Global	Global
Lin.	Coeff	rd/mm	0,027	0,037	0,024	0,013				
	From		CEL	CEL	CEL	CEL				
	Contrib	rd	5,4E-04	7,4E-04	4,8E-04	2,6E-04				
Ang	Coeff	rd/rd	0,006	2,07	0,976	2	1	1	1	1
	From		CEA	CEA	CEA	CEA	COA	CVA	VFA	FTA
	Contrib	rd	6,0E-07	2,1E-04	9,8E-05	2,0E-04	1,0E-04	7,0E-04	5,0E-04	5,0E-04
WorstCase		***4,3E-03rd***								
RSS		***1,5E-03rd***								

Band 8			Horn	Grid	Mirr1	Mirr2	Global	Global	Global	Global
Lin.	Coeff	rd/mm	0,019	0,019	0,037	0,021				
	From		CEL	CEL	CEL	CEL				
	Contrib	rd	3,8E-04	3,8E-04	7,4E-04	4,2E-04				
Ang	Coeff	rd/rd	0,008	0,66	3,36	2	1	1	1	1
	From		CEA	CEA	CEA	CEA	COA	CVA	VFA	FTA
	Contrib	rd	8,0E-07	6,6E-05	3,4E-04	2,0E-04	1,0E-04	7,0E-04	5,0E-04	5,0E-04
WorstCase		***4,3E-03rd***								
RSS		***1,5E-03rd***								

Band 9			Horn	Grid	Mirr1	Mirr2	Global	Global	Global	Global
Lin.	Coeff	rd/mm	0,039	0,039	0,064	0,039				
	From		CEL	CEL	CEL	CEL				
	Contrib	rd	7,8E-04	7,8E-04	1,3E-03	7,8E-04				
Ang	Coeff	rd/rd	0,004	1,63	4,43	2	1	1	1	1
	From		CEA	CEA	CEA	CEA	COA	CVA	VFA	FTA
	Contrib	rd	4,0E-07	1,6E-04	4,4E-04	2,0E-04	1,0E-04	7,0E-04	5,0E-04	5,0E-04
WorstCase		***6,2E-03rd***								
RSS		***2,2E-03rd***								

Band 10			Horn	Grid	Mirr1	Mirr2	Global	Global	Global	Global
Lin.	Coeff	rd/mm	0,02	0,02	0,043	0,026				
	From		CEL	CEL	CEL	CEL				
	Contrib	rd	4,0E-04	4,0E-04	8,6E-04	5,2E-04				
Ang	Coeff	rd/rd	0,007	0,67	3,3	2	1	1	1	1
	From		CEA	CEA	CEA	CEA	COA	CVA	VFA	FTA
	Contrib	rd	7,0E-07	6,7E-05	3,3E-04	2,0E-04	1,0E-04	7,0E-04	5,0E-04	5,0E-04
WorstCase		***4,6E-03rd***								
RSS		***1,6E-03rd***								

Evaluation of results.

For bands 1–4, the most important single cause of misalignment is between the cartridge and the vacuum vessel, which introduces an internal break in the optical train. For higher frequency bands, and with the assumed values, there are comparable contributions from internal cartridge alignment and cartridge/dewar/telescope alignment. Band 9 has a higher estimate of misalignment because of the relatively fast optics that it uses.

The model used for internal cartridge optics tolerancing may be overly simplistic, in that it assumes that there is just one intermediate support part between any optical element and the 4K plate. A more

complex construction might still be consistent with the above error estimate if the attachment points/planes of individual elements would be machined on a permanently assembled support structure, thereby eliminating individual tolerances in the mechanical chain. The pressure deformation of the vacuum vessel might be compensated in the construction, either a priori from FEA modeling, or after evaluation of a prototype; but this is not essential to meet the goals, as will be seen below.

All individual tolerances used as input in the calculation need to be confirmed by the respective groups in charge.

Worst-case or RSS? If the analysis would apply to a single instrument, the worst-case analysis would maybe be more appropriate. However, the telescopes will operate most of the time in an array, and the figure of merit is the array efficiency. Since the efficiency of an individual antenna degrades quadratically with the aperture plane offset, the effective apertures for two antennas and the corresponding baseline can be written respectively as:

$$A_i = A_0\left(1-k\left(\frac{\theta_i}{\theta_0}\right)^2\right) \quad i=1,2$$

$$A_{12} = \sqrt{A_1 A_2} \approx A_0\left(1-\frac{1}{2}k\left(\frac{\theta_1^2+\theta_2^2}{\theta_0^2}\right)\right)$$

where θ_0 is the misalignment for which the reference degradation k is reached. The expectation value of the baseline effective aperture is:

$$\langle A_{12}\rangle = A_0\left(1-k\left(\frac{\theta_{RSS}}{\theta_0}\right)^2\right)$$

where I have made the implicit assumption that the individual positioning tolerances are in fact rms values, which is pessimistic if they are actually maximum values (as they should be for mechanical tolerances).

This said, if we examine the RSS misalignment values for each of the ten bands, and multiply them by $\sqrt{2}$ to account for the two possible misalignment directions, we can see that they are safely below the critical value $\theta_0 = 5.5\ mrad$.

4. Co-alignment of orthogonal polarizations in focal plane

In this part, using the same estimates for linear and angular positioning errors of individual elements, and again using the matrices P (see Appendix A) I estimate the misalignment in the focal plane of the two beams of one channel. This concerns only bands 7 and above, since bands 1-6 are planned to use OMT's, that in principle guarantee the co-alignment of the two orthogonal polarizations. Remember that in this work, I consider only the propagation of the fundamental Gaussian mode; physical optics calculations by Tham and Withington do show small offsets between orthogonally polarized beams propagating through off-axis mirrors. The results are listed in Table 2.

Table 2. Estimates of the lateral misalignment of the two orthogonally polarized beams, for each band, expressed in the focal plane, worst-case and RSS, in mm and as a fraction of the FWHM at mid-band.

Band 7			Horn	Mirr1	Grid
Lin	Coeff	mm/mm	0.91	3	3.8
	From		CEL	CEL	CEL
	Contrib	mm	0.0182	0.06	0.076
Ang	Coeff	mm/rd	54	218	24
	From		CEA	CEA	CEA
	Contrib	mm	0.0054	0.0218	0.0024
WorstCase		**0.184 mm**		**0.025 beam**	
RSS		**0.101 mm**		**0.014 beam**	

Band 8			Horn	Grid
Lin	Coeff	mm/mm	1.49	1.5
	From		CEL	CEL
	Contrib	mm	0.0298	0.03
Ang	Coeff	mm/rd	53	159
	From		CEA	CEA
	Contrib	mm	0.0053	0.0159
WorstCase		**0.081 mm**		**0.015 beam**
RSS		**0.045 mm**		**0.008 beam**

Band 9			Horn	Grid
Lin	Coeff	mm/mm	2	2
	From		CEL	CEL
	Contrib	mm	0.04	0.04
Ang	Coeff	mm/rd	25	134
	From		CEA	CEA
	Contrib	mm	0.0025	0.0134
WorstCase		**0.096 mm**		**0.026 beam**
RSS		**0.058 mm**		**0.016 beam**

Band 10			Horn	Grid
Lin	Coeff	mm/mm	1.8	1.8
	From		CEL	CEL
	Contrib	mm	0.036	0.036
Ang	Coeff	mm/rd	48	159
	From		CEA	CEA
	Contrib	mm	0.0048	0.0159
WorstCase		**0.093 mm**		**0.034 beam**
RSS		**0.054 mm**		**0.019 beam**

The co-alignment of the two beams of one band remains — under the adopted hypotheses — always better than 3.5% of the FWHM.

5. Aberrations introduced by misalignments

With nominal alignment, the off-axis elliptical mirrors couple (almost) exactly the phase of the incident and reflected fundamental Gaussian beams; losses (i.e., coupling to higher order modes) come from the mismatch of the amplitude (and polarization) patterns. Under nominal conditions, the centers

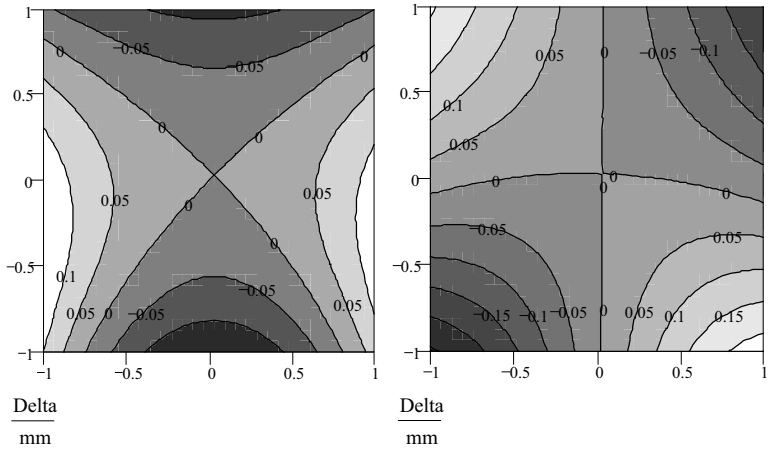

Figure 4. Examples of phase error patterns for misalignments of the incident wavefront center of curvature, resp. in the plane of reflection, and in the perpendicular direction. The contours are labeled with the path error (mm); the mirror coordinates are arbitrary.

of curvature of the incident and reflected wavefronts coincide with the foci of the ellipsoid. This is equivalent to the condition of equal optical path for all contributing rays.

In a misaligned system, that condition is not met. For a given position of the incident wavefront's center of curvature, a reflected center of curvature can be defined such that the optical path is constant (versus the reflection point on the mirror) up to tilt and focus terms; it is simply the paraxial geometrical optics image. Higher order residuals induce a loss of amplitude (and power) for the propagation of the fundamental Gaussian mode.

For a given lateral misalignment of the incident center of curvature with respect to the first focus of the ellipsoid, one can compute the phase error across the surface of the mirror (dominated by astigmatism).

Two approaches can be taken to estimate the amplitude loss of the reflected beam; they are briefly described in Appendix B. Here, I adopted the most severe one, based on the amplitude-weighted rms phase error.

The results are given in Table 3, giving for each band, and for each mirror, the degree of lateral misalignment leading to a power loss of 1% in the fundamental mode.

Table 3. Amount of lateral misalignment inducing a power loss of 1% in the fundamental mode, through phase aberrations.

Band	Allowed misalignment (mm)	
	Mirror 1	Mirror 2
4	13	N/A
6	2.4	4
7	1.9	5.7
8	2.6	1.7
9	0.65	0.54
10	1.3	0.67

These values are much larger than either achievable tolerances or critical individual tolerances derived in section 3.1 and displayed in figures 2 and 3.

6. Phase across the primary beam

The discussion in this section stems from a concern expressed by P.Napier. Since then, it seems that the issue might be resolved by suitable calibration and data processing [S.Guilloteau, private

communication]; however, that is not officially established, therefore I felt it would be appropriate to give a presentation of the argument.

An elementary interferometric observation provides an estimate (at one point in the UV plane) of the Fourier transform of the product of the sky brightness and the voltage patterns of the two antennas of one baseline. In most, if not all, of radio interferometric work so far, after the raw sky brightness is reconstructed from the UV data, it is corrected for the power pattern, often using a Gaussian ansatz for a "typical" power pattern of an antenna of the array. The phase across the primary beam is *assumed* to be constant. The latter is true provided the (complex) aperture illumination is azimuthally symmetric. Conversely, an aperture plane misalignment will result in a non-uniform phase across the primary beam, leading to imaging errors.

I have performed a numerical simulation of the voltage pattern for a Gaussian illumunation, having a 12dB taper, and offset by 10% of the aperture radius. The phase of the amplitude pattern is close to 0.1rd at the half-power points. If we denote by a the amplitude pattern, normalized to 1 at boresight, and a_0 the same with flat phase, the error in apparent amplitude $|a - a_0|$, is maximum close to the half-power points ($a_0 = 2^{-1/2}$), where $|a - a_0| \approx 0.07$. Since the effect is clearly linear versus the aperture plane offsets, these numerical results can be generalized to :

$$\phi_{3dB} \approx \delta x_s / r_s$$
$$|a - a_0|_{3dB} \approx a_{0,3dB} \times \phi_{3dB}$$

where $\delta x_s / r_s$ is the normalized aperture plane misalignment.

Following a remark by R.Lucas, the errors in the imaginary part of the apparent amplitude — resulting from aperture plane misalignment — can be compared with the errors in the real part — resulting from focal plane, or pointing errors. Both should play the same role in imaging, in particular mosaicing.

The technical *requirement* for pointing, flowing from the scientific *requirement* for high fidelity imaging, is that the pointing accuracy should be 6%HPBW (Project Book, Chap 2, Table 2.1). The resulting antenna performance requirement is 0.6" pointing accuracy (Chap 2, Table 4.1). For a pointing error that is a fraction f of the HPBW, the error in the apparent amplitude a of a point source observed at the half-power point is:

$$\delta a = \sqrt{2}\,\mathrm{Ln}(2)\, f = 0.98 f \approx f$$

Based on the scientific *requirement*, $f = 0.06$, this leads to $\delta a \approx 0.06$, consistent with the magnitude in the imaginary part of a resulting from the spec $\delta x_s / r_s \leq 0.088$ derived in section 3 of the present report, from the consideration of minimal loss of on-axis efficiency.

However, the actual antenna built has an absolute pointing accuracy, independent of wavelength, which is a smaller fraction f of HPBW at longer wavelengths. Understandably, the scientists would like to benefit from the maximum possible imaging quality at these longer wavelengths, and therefore asked to lower accordingly the ceiling on the error on Im(a), resulting in tighter specs for the aperture plane alignment at low frequencies. This summarized graphically in Figure 5.

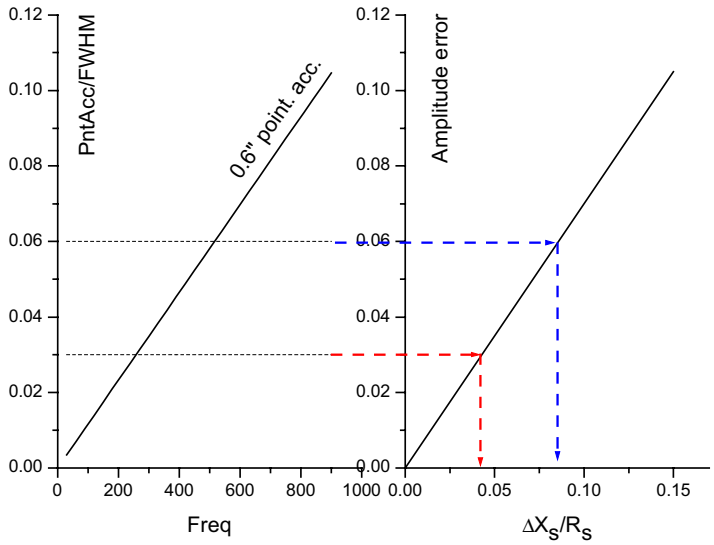

Figure 5. Relation between relative pointing accuracy, amplitude error (real or imaginary part), and consistent spec for aperture plane alignment. See text for discussion.

However:

- Pointing errors (after pointing corrections) are random, while
- The phase across the primary beam is a systematic error that, if stable, can in principle be calibrated out

Accordingly, and following a preliminary indication that the primary beam phase can indeed be corrected for, I propose to leave the aperture plane alignment spec at $\delta x_s / r_s \leq 0.09$.

7. Conclusions

The sensitivity of aperture and focal plane misalignments of ALMA FE optics has been studied. Four performance criteria have been taken into account: a) loss of on-axis efficiency from aperture plane misalignment; b) focal plane co-alignment of the two beams of each band; c) aberrations when off-axis mirrors operate between wavefronts not centered on the foci of the ellipsoid; d) non-uniform phase across the primary beam resulting from aperture plane misalignment.

It is found that the driving consideration is aperture plane misalignment, in relation with aperture efficiency. Assuming reasonable values for the various sources of misalignment, it is found that the performance criteria that were set as goals can be met.

8. References

[1] Lamb, J. et al. ALMA memo 362. http://www.alma.nrao.edu/memos/

[2] ALMA Project Book. http://www.alma.nrao.edu/projectbk/construction/

[3] Tham, C.Y. and Withington, S.. Receiver Optics Design: Electromagnetic Analysis. Draft report Sep-2001.

A.1. Perturbation of chief ray from misalignments

Two types of perturbations to perfect alignment are considered: breaks and isolated displacements. The difference between these two types of misalignments is illustrated in Figure A-1, in the case of an inline lens system.

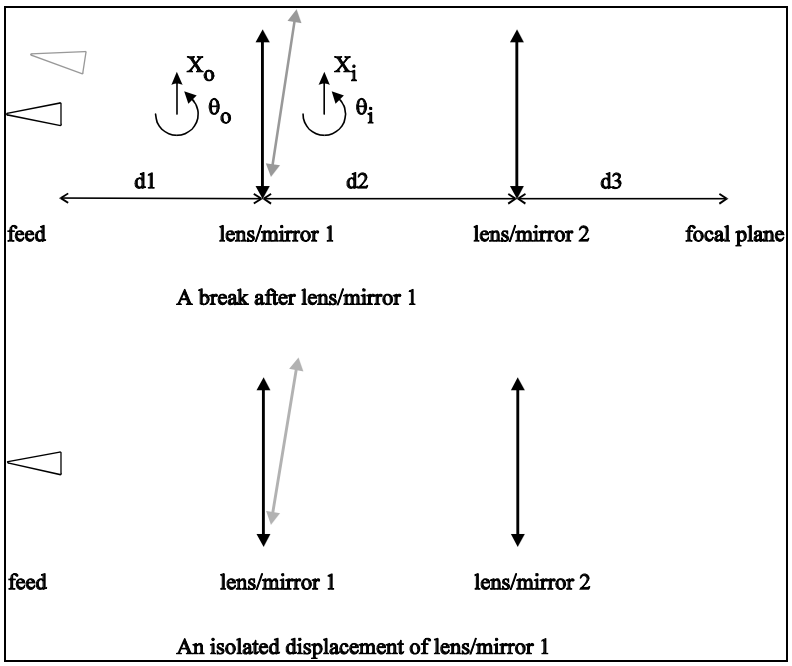

Figure A-1. Definition of two types of misalignments.

Note: The displacement (shift+rotation) of an optical element is reckoned in its image (**i**) space in the case of a break, and in its object (**o**) space in the case of a displacement. The center of rotation is defined in either case at the optical center of the element. These two frames are distinct only in the case of mirrors, of course.

In the case of a break, the (X,θ) displacement is propagated through the rest of the system, for example, in the case of a break after lens/mirror 1:

$$P := \text{Space}(d3)\cdot\text{Lens}(f2)\cdot\text{Space}(d2)$$

where Lens(f) is the usual ABCD matrix for a thin lens/mirror, and Space(d) the matrix for free propagation over a distance d.

In the case of an individual displacement of an optical element, we need the perturbation of the image ray as a function of the displacement of that element:

$$\begin{pmatrix} X_i \\ \theta_i \end{pmatrix} := \begin{pmatrix} 1-\cos(\alpha) & 0 & \sin(\alpha) \\ -\frac{1}{f} & 2 & 0 \end{pmatrix} \cdot \begin{bmatrix} X_o \\ \theta_o \\ Z_o \end{bmatrix}$$

in the case of a mirror (the only case where a Z-displacement along the ray path is significant); and:

$$\begin{pmatrix} X_i \\ \theta_i \end{pmatrix} := \begin{pmatrix} 0 & 0 \\ \frac{1}{f} & 0 \end{pmatrix} \cdot \begin{pmatrix} X_o \\ \theta_o \end{pmatrix}$$

in the case of a lens (insensitive to lens tilt in the paraxial approximation); in either case, the perturbation is then propagated through the rest of the system.

The end result is a 2×2 matrix *P* (2×3 for the individual displacement of a mirror) that relates the X,θ displacement of the beam in the focal plane to the misalignment parameters. These matrices have been

used in section 3.2 to derive the global budget, and in section 4 to study the co-alignment of the two orthogonal polarizations. The tolerances for individual displacement that would, *alone*, use up the alignment tolerance, shown in Figs 2, 3 (section 3.1) were derived from the following equations:

$$Tol(X) = \left|P_{2,1}\right|^{-1} \times \theta_C$$

$$Tol(\theta) = \left|P_{2,2}\right|^{-1} \times \theta_C$$

$$Tol(Z) = \left|P_{2,3}\right|^{-1} \times \theta_C \qquad \text{(only in the case of a mirror's individual displacement)}$$

A.2. Loss from phase aberration: amplitude versus power weighting

1. Main reflector, loss of on-axis efficiency.

Let $a(x,y)$ be the amplitude across the aperture, and let's assume for the unperturbed illumination that a is real positive (flat phase), and that the perturbed illumination is described by a phase distribution ϕ with zero mean value. The relative aperture efficiency is given by:

$$A_{eff} = \left| \iint_A a \exp(i\phi)\, dx\, dy \Big/ \iint_A a\, dx\, dy \right|^2$$
$$\approx 1 - \iint_A a\,\phi^2\, dx\, dy \Big/ \iint_A a\, dx\, dy$$

2. Arbitrary refocusing mirror, mode coupling

The amplitude coupling coefficient between modes a_1 and a_2, with phase aberrations is given by:

$$\gamma = \frac{\iint a_1\, a_2^* \exp(i\phi)}{\sqrt{\iint a_1\, a_1^*}\sqrt{\iint a_2\, a_2^*}}$$

Assume that without the phase perturbation, the mirror gave perfect coupling, i.e. $a_1 = a_2$, and let: $a = \left|a_1\right| = \left|a_2\right|$. Then the power coupling amplitude coupling with phase errors is given by:

$$\left|\gamma\right|^2 \approx 1 - \frac{\iint a^2\phi^2}{\iint a^2}$$

3. Discussion

A comparison between the two equations for loss of efficiency can be made only when the output beam is focused at infinity.

In case the phase perturbations have uniform properties over the aperture (magnitude, scale), and the scale is small w/r to the scale of the field amplitude, the two equations give the same result, which is $1 - \left\langle \phi^2 \right\rangle$. This is consistent with the fact that, under such conditions, the "main beam" loses amplitude, but retains its shape; so, the same number measures the loss of on-axis efficiency and loss of mode (power) coupling.

Differences arise when the scale-length of ϕ is comparable with that of a. Rather than scattering power into a wide error beam, a more appropriate description is that the main beam is distorted. Then the decrease in fundamental mode power need not be the same the decrease in on-axis effective area.

When discussing losses at an arbitrary point in telescope optics that is not the main reflector aperture, on-axis efficiency does not have a clear meaning, and the mode coupling equation is probably more meaningful.